DEVELOPMENT OF A FINITE ELEMENT MODEL FOR FLEX-PLI

Yuji Kikuchi
Honda R&D Co., Ltd.
Japan
Yukou Takahashi
Honda R&D Americas, Inc.
Fumie Mori
PSG
Paper Number 05-0287

ABSTRACT

A finite Element (FE) model of the next-generation flexible pedestrian leg-form impactor (Flex-PLI) developed by the Japan Automobile Manufacturers Association (JAMA) and Japan Automobile Research Institute (JARI) was developed in this study. The Flex-PLI is intended to be used in evaluating safety of car front structures against the lower limbs of pedestrians. A 3D geometry of each part was reproduced in PAM-CRASH™ based on drawings of the Flex-PLI. For material characterization, the stress-strain characteristics were determined from the results of the material tests on each individual component, with the strain rate dependency of the material taken into account. The results of the dynamic 3-point bending test for the thigh and leg and the dynamic 4-point bending test for the knee joint performed by JARI were used to validate the model. The validation results showed that the computer simulation results for the force-deflection response of the thigh and leg as well as the moment-angle response of the knee joint agreed well with the test results. Impact tests against vehicles at 40 km/h were reproduced using the model, and the results were compared with the test results. The results of the comparison showed that the kinematics of the Flex-PLI could be reproduced by the computer simulation. It was also found that the bending moment of the thigh and leg as well as the elongation of the ligament cables of the knee joint could be accurately reproduced.

INTRODUCTION

According to pedestrian accident data, pedestrians account for approximately 30% of fatalities in traffic accidents in Japan. For this reason, pedestrian protection along with occupant protection is considered as an important issue in the improvement of vehicle safety [1]. Distribution of AIS 2+ injuries from the Pedestrian Crash Data Study (PDCS) database in the U.S. shows that the frequency of injuries to the head and lower limb dominates as shown in Figure 1. Because injuries to the head are often fatal, head injuries are considered as the most serious injuries. Lower limb injuries are also important because of their long-term consequences and high social costs.

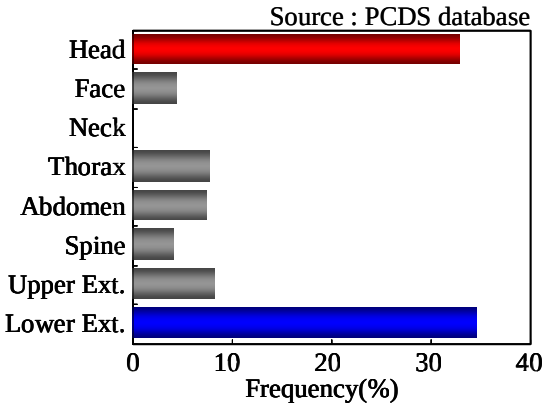

Figure 1. Distribution of AIS2+ pedestrian injuries by body region

In order to reduce these injuries in pedestrian accidents, the European Enhanced Vehicle-safety Committee (EEVC) Working Group 17 has proposed a vehicle test procedure employing a head-form impactor, upper leg-form impactor, and leg-form impactor. For the leg-form impact test, a leg-form impactor developed by the Transportation Research Laboratory (TRL) known as TRL-PLI has normally been used [2]. However, it has been pointed out that it is necessary to improve the biofidelity of the TRL-PLI and the validity of the injury criteria [3]-[5]. Accordingly, a flexible-pedestrian leg-form impactor (Flex-PLI) has been developed jointly by JAMA and JARI as a next-generation impactor that has greater biofidelity. The thigh, knee joint and leg of the Flex-PLI have been built of flexible structure in order to obtain more realistic kinematics of the human lower limb. The published test results using Post Mortem Human Subjects (PMHS) were used to validate the dynamic response of the limb [6]-[8].

In this study, an FE model for the Flex-PLI was developed for use in vehicle development for improved safety of vehicle front structures against pedestrian lower limbs.

MODEL DESCRIPTION

As shown in Figure 2, the Flex-PLI consists of three segments, the thigh, knee joint, and leg. The thigh and leg were made flexible in order to reproduce deflection of the human bones. The knee joint of the Flex-PLI has a simplified structure that represents geometry of bones and ligaments. However, the knee joint is capable of reproducing bending and shear in human knee joint due to lateral impact from a vehicle to the lower limb of a pedestrian.

The 3D geometry of each component of the Flex-PLI was precisely reproduced in PAM-CRASH^{TM} based on the drawings of the Flex-PLI [9]. Since the fairly rigid steel and aluminum parts were modeled as rigid bodies, it was necessary to determine mass and moment of inertia of those parts for the rigid body definitions. Those numbers were determined by importing the 3D geometry of the parts into PAM-GENERIS^{TM} and giving appropriate density for the parts [10]-[12].

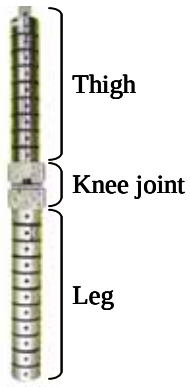

Figure 2. Flex-PLI

Thigh and Leg

Figure 3 shows the bony structure of the thigh and leg. The bony structure is assembled by surrounding the bone core with the core spacer and core binder, fixing these parts together with adhesive, inserting them into the exterior housing, then bolting them from outside of the exterior housing, as shown in the cross-sectional diagram (Figure 4). By tightening the bolt, the core binder is pushed against the core spacer compressing it, after which the exterior housing is fixed to the bone core. The exterior housings are piled up axially with the rubber spacers in between. The thigh and leg are with nine and eleven exterior housing blocks, respectively. Figure 5 shows the FE model for the thigh and leg. Since the resin bone core, core spacer and rubber spacer are subjected to large deformation, those parts were modeled as deformable solid elements. The fairly rigid steel and aluminum parts such as the exterior housing and core binder were modeled as rigid bodies. The cross section of

the bone core is shown in Figure 6. Since the length of one side of the bone core is not long enough to provide practical level of time integration step in PAM-CRASH™ (estimated time step was 0.575 μ sec), it was decided to simplify the cross section with a rectangular shape in such a way that the areal moment of inertia is conserved as shown in Figure 7. This resulted in the time step of 1.04 μ sec and significantly reduced CPU time.

The constraints used in the model for each part were determined based on the actual Flex-PLI assembly procedure. Because the core spacer and core binder are glued to the bone core and core spacer, respectively, there is no degree freedom on the interface. Consequently, Sliding Interface Type 10 (Tide Contact) was used on the contact surface between the bone core and the core spacer as well as the contact face between the core spacer and core binder. A joint element with all degrees of freedom fixed was used to connect the core binder to the external housing. Since the rubber spacer is glued to one side of the exterior housing, Sliding Interface Type 10 was applied to define the interface between those parts. On the other side of the rubber spacer, which is not glued to the exterior housing, Sliding Interface Type 33 was used to define the contact with the exterior housing. This modeling reproduced the deformation of the rubber spacer by selecting appropriate contact models that accurately represent the actual interface conditions.

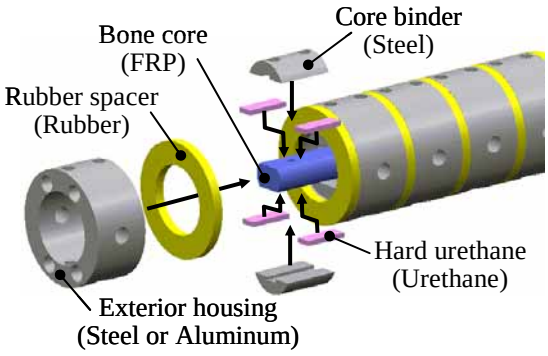

Figure 3. Structure of thigh and leg

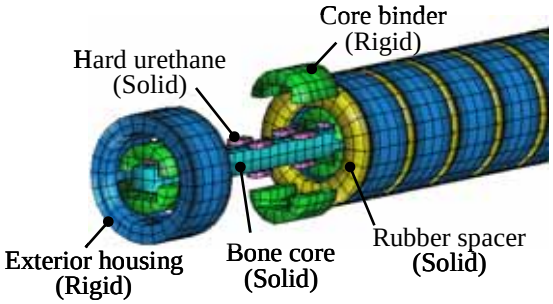

Figure 5. Thigh and leg model

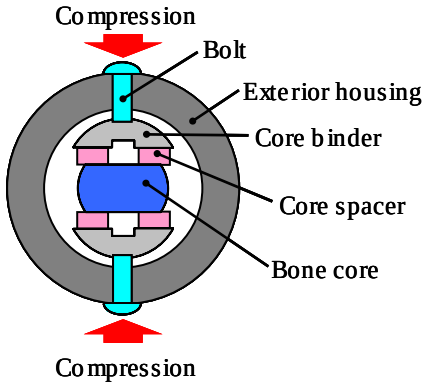

Figure 4. Section of thigh and leg

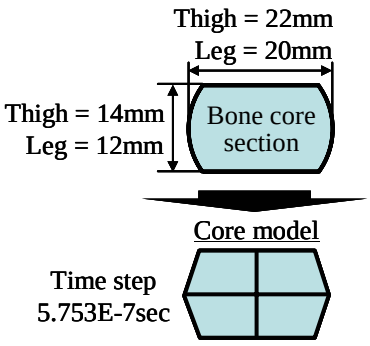

Figure 6. Bone core section and model section

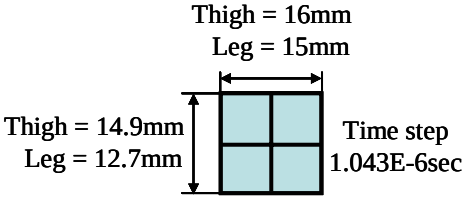

Figure 7. Section of bone core model

Knee Joint

Figure 8 shows the structure of the knee joint for the Flex-PLI. The upper and lower tibia condyle surface are glued to the lower tibia condyle surface and the tibial condyle, respectively. Knee springs that determine the tensile properties of the knee ligaments are installed in the femoral and tibial condyle. Knee cables simulating the knee ligaments pass through the inside of the knee springs, connecting the femoral condyle to the tibial condyle to configure the knee joint.

The FE model for the knee joint is shown in Figure 9. Rigid aluminum components such as the femoral condyle, upper tibia condyle surface, and tibial condyle were modeled as rigid bodies while the lower tibia condyle surface, which is made of hard urethane, was modeled using solid elements. All nodes were shared on the two interfaces between the upper and lower tibia condyle surface and the tibial condyle. Each pair of the knee springs and knee cable representing four major ligaments in a human knee (Anterior Cruciate Ligament; ACL, Posterior Cruciate Ligament; PCL, Medial Collateral Ligament; MCL, Lateral Collateral Ligament; LCL) was lumped together and modeled using one single bar element as shown in Figure 10. The material properties of the springs were modeled using Material Type 205 in PAM-CRASH™.

Flesh

As shown in Figure 11, Neoprene sheets with the thickness of 10 mm and 5 mm are wrapped around the thigh, knee joint and leg as the flesh of the Flex-PLI. In addition, on the side of the impactor that is supposed to be impacted by a vehicle, a rubber sheet with the thickness of 5 mm was inserted between the two Neoprene layers. Those sheets were modeled using solid elements with exactly the same thickness as shown in Figure 12. For defining contact of the flesh to the thigh, leg, and knee joint, Sliding Interface Type 33 was used in order to accurately reproduce motion of the flesh relative to the thigh, leg, and knee joint.

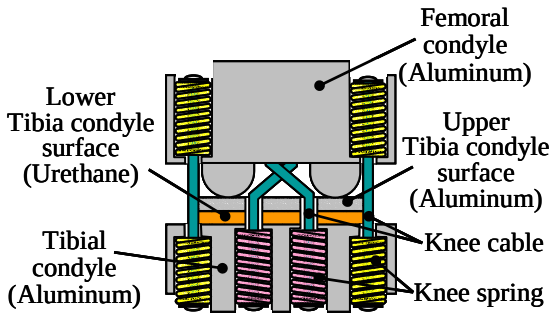

Figure 8. Structure of knee joint

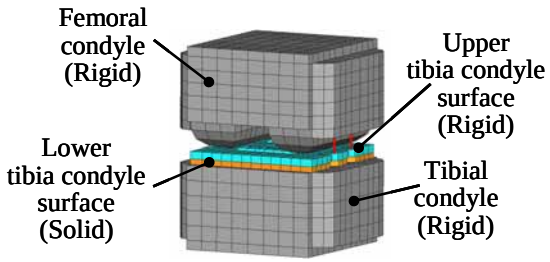

Figure 9. Knee joint model

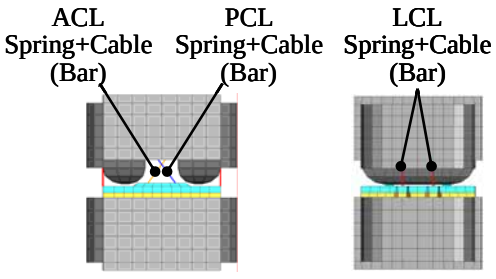

Figure 10. Knee spring and ligament model

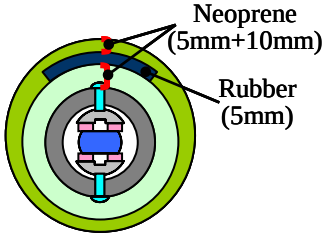

Figure 11. Structure of flesh

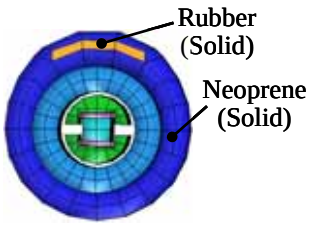

Figure 12. Section of flesh model

VALIDATION OF MATERIAL PROPERTIES

In order to ensure accuracy of the model, the stress-strain characteristics of the material models for the resin parts were determined by running some material tests using those parts. The target for the model validation was that the computer simulation results fall within ±10% of the average experimental results.

Bone Core

The bone core model was validated against the results of the quasi-static and dynamic 3-point bending tests performed by Konosu et al. [6]. Figure 13 shows the test set-up used by Konosu et al. The bone core was simply supported using circular cylinders with 50 mm diameter placed underneath its both ends. The span length was set at 250 mm. An impactor with 43.2kg weight and 50 mm diameter tip applied load at mid-span in quasi-static condition (0.1mm/s) as well as at impact speeds of 0.99 m/s and 1.44 m/s to obtain force-deflection response. Since the rate dependency was not observed in the measured force-deflection response, Material Type 16 in PAM-CRASH™ was used to apply linear elastic material model. Figure 14 shows a set-up of the model that simulates the 3-point bending test conducted by Konosu et al. The results of the comparison between experiment and computer simulation are shown in Figure 15 and 16 for the thigh and leg bone core, respectively. The computer simulation results fell within ±10% of the results of the test results in all loading rates, indicating good agreement. The results also suggest that the model with a simplified cross section can yield good results as long as the areal moment of inertia is maintained.

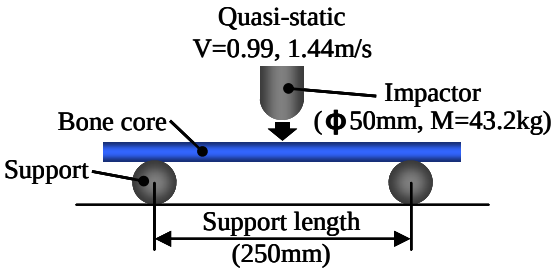

Figure 13. 3 point bending test setup for bone core

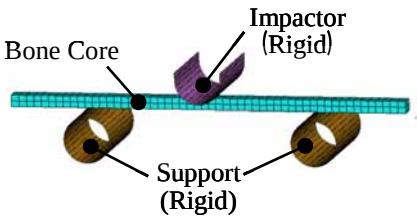

Figure 14. Model setup for bone core validation

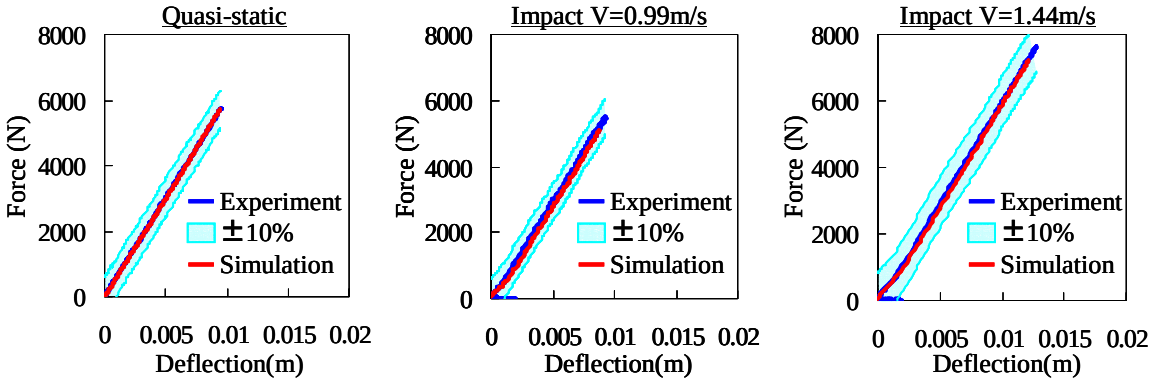

Figure 15. Comparison between load-deflection response and simulation result of thigh bone core in 3 pint bending

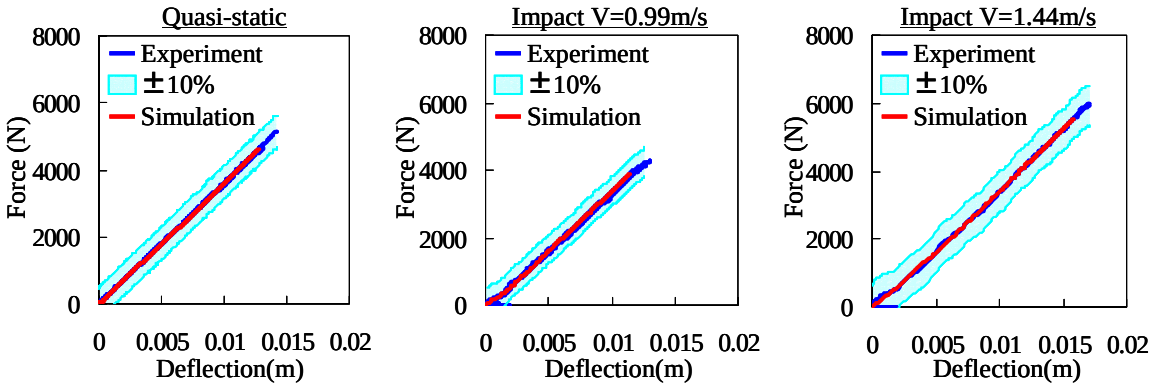

Figure 16. Comparison between load-deflection response and simulation result of leg bone core in 3 pint bending

Other Resin Components

The mechanical characteristics of the resin components such as the core spacer and rubber spacer of the thigh and leg, the lower tibia condyle surface in the knee joint, and the flesh were measured in this study. As shown in Figure 17, compression tests with the impactor of 41.6 kg weight and 50 mm diameter tip were run against a test specimen made of each material, and the dynamic foece-deflection responses were measured. Similarly, quasi-static compression tests were also performed in order to obtain quasi-static force-deflection responses that were used to determine stress-strain relationship for the materials.

The degree of strain rate dependency can be evaluated by comparing the quasi-static and dynamic force-deflection responses of each material. Since the test results showed that the materials tested were rate dependent, strain rate dependent material models were used. As shown in Figure 18, computer simulation models that simulate the material tests were built in order to determine material model parameters. Force-deflection responses from the quasi-static compression tests were converted into stress-strain relationships. The stress was obtained from the compressive force divided by the initial cross sectional area of the test specimen, and the strain was calculated from the displacement of the impactor divided by the initial thickness of the test specimen. Material Model Type 21 (Solid element) in PAM-CRASH™ was used to characterize the materials. As for the strain rate dependency, Cowper-Symonds strain rate model was used and the strain rate parameters for this model were determined in such a way that the computer simulation results best match the test results. Figure 19 shows the results of a comparison between experiment and computer simulation in quasi-static compression for each material. The results showed that the stress-strain relationships estimated from the force-deflection responses were valid. Once quasi-static stress-strain relationships were established, strain rate parameters were determined so that the computer simulation results for dynamic compression of the materials agree well with the test results. As shown in Figure 20, the simulation results were within ±10% of the test results, thus indicating that the strain rate parameters used in the models accurately characterize the strain rate dependency of the actual materials.

VALIDATION OF THIGH AND LEG MODEL

Since the results of the material model validation of the bone core and each resin part confirmed accuracy of the material models, the dynamic response of the

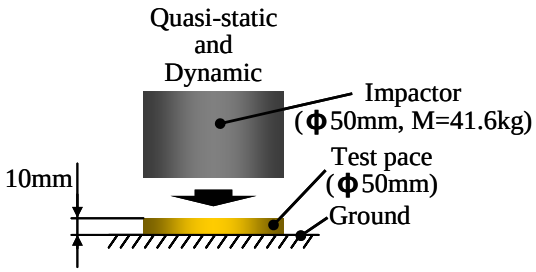

Figure 17. Compression test setup for resin materials

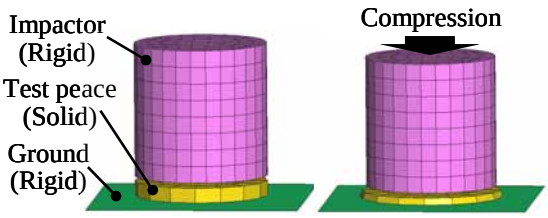

Figure 18. Compression test model setup for resin materials

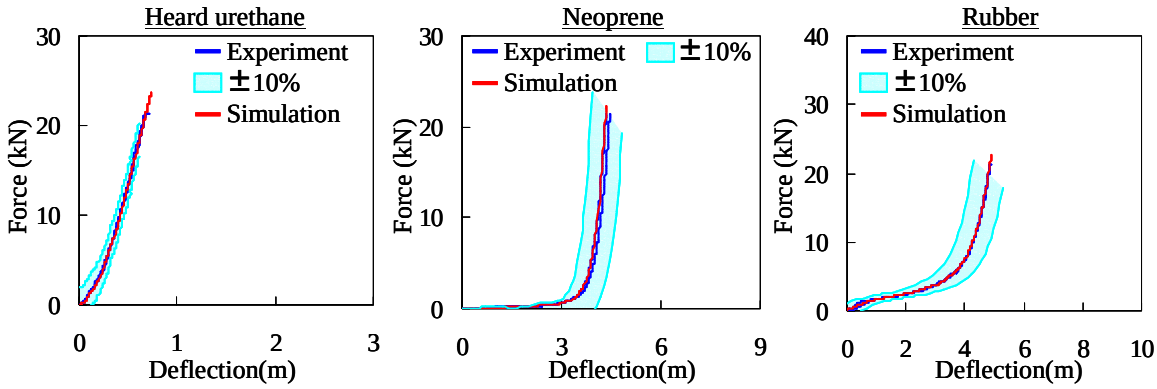

Figure 19. Comparison between load-deflection response and simulation result of resin materials in quasi-static compression test

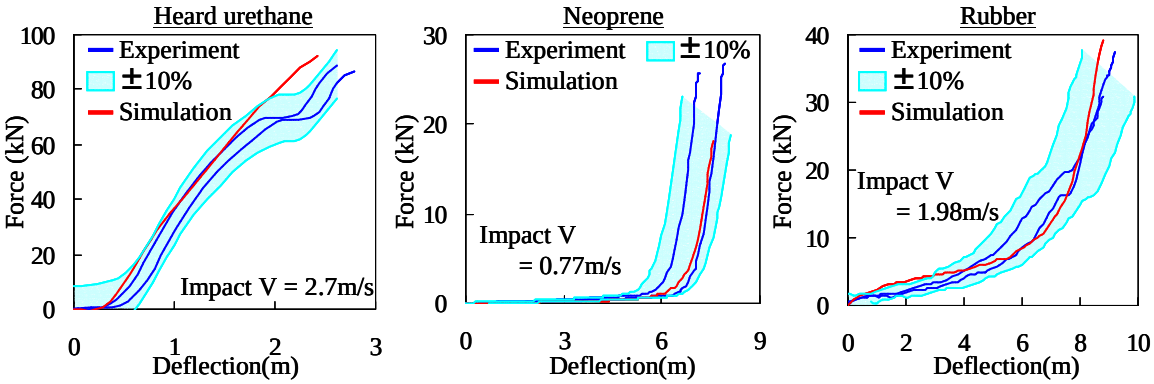

Figure 20. Comparison between load-deflection response and simulation result of resin materials in dynamic compression test

thigh and leg model was validated as the next step. In the model validation, the results of the 3-point bending tests for the thigh and leg performed by Konosu et al. [7][8] were used. As shown in Figure 21, both ends of the thigh or leg were simply supported. An impactor that weighed 67.8 kg was impacted against the mid-shaft of the thigh or leg in lateromedial direction at an impact speed of 1.0 m/s, and the force-deflection response was measured. The computer simulation model shown in Figure 22 was created using the thigh and leg model to simulate the experiment, and the test results were compared with the computer simulation results. Figure 23 shows the results of the comparison between the test and computer simulation for the force-deflection response. The figure shows that the computer simulation results are within ±10% of the test results, thus confirming that the model can accurately reproduce the dynamic response of the thigh and leg. As can be seen from the cross-section of the

deformed thigh model in Figure 24, the rubber spacer and core spacer of each part are compressed, the internal bone core deflects smoothly without large local deformation, the exterior housing and core binder follow the bone core, and the overall deflection of the bone structure is reproduced. By determining constraints for the model of each part in such a way that the constraint precisely represents the actual assembly procedure, it was possible to simulate the response of the thigh and leg as a result of accurate reproduction of load paths inside the exterior housings.

VALIDATION OF KNEE JOINT MODEL

To validate the knee joint model, the results of the 4-point bending test of the knee joint performed by Konosu et al. [7] were used. The set-up used by Konosu et al. is shown in Figure 25. A load cell and a shaft were installed on both sides of the knee joint, and both ends of the knee test specimen assembly were rigidly attached to a support roller to provide simply supported condition. A fork with two prongs weighing 74.5 kg applied load onto the knee joint test specimen assembly at a speed of 1.4 m/s in such a

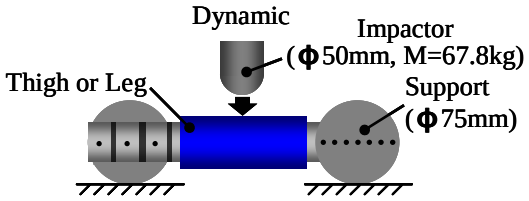

Figure 21. Dynamic 3 point bending test setup for thigh and leg

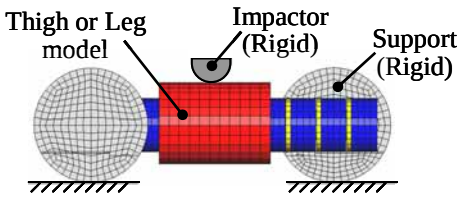

Figure 22. Dynamic 3 point bending model setup for thigh and leg

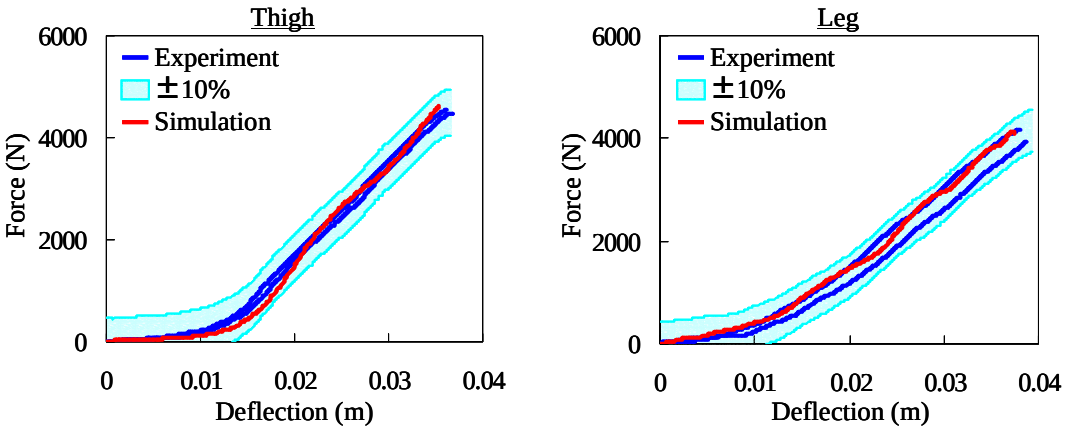

Figure 23. Comparison of load-deflection response of thigh and leg between experiment and simulation

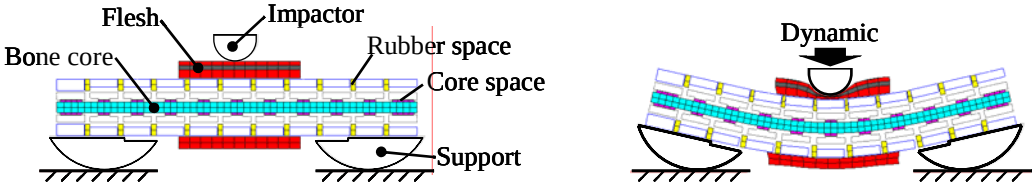

Figure 24. Kinematics of the thigh model for 3 point lateral bending test simulation

way that the knee bends in valgus. The moment-angle response of the knee joint was then measured. The definition of the knee moment was the average moment from the load cells installed on the inferior and superior side of the knee joint. A computer simulation model that simulates the experiment was created as shown in Figure 26 in order to validate the dynamic response of the knee joint. Figure 27 shows the comparison between experiment and computer simulation. The bending moment in the initial phase generated by the inertial effect was higher for computer simulation. However, the bending moment in the subsequent phase, which is primarily from the knee bending response, agreed well between the test and computer simulation, confirming that the dynamic response of the knee joint can be reproduced by the model.

Based on the above shown validation results, high accuracy of the model was confirmed in component level.

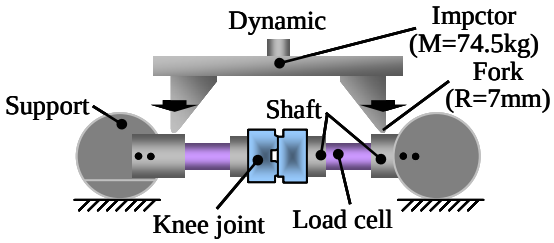

Figure 25. Dynamic 4 point test setup for knee joint

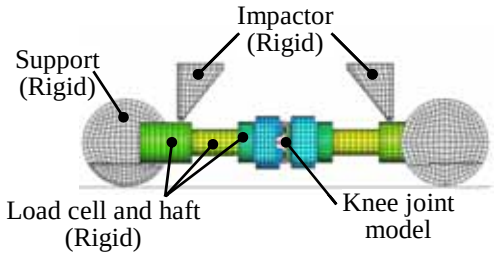

Figure 26. Dynamic 4 point model setup for knee joint

MODEL VALIDATION AGAINST VEHICLE IMPACT TEST

Vehicle impact tests using the Flex-PLI were performed and the results were used to validate the model in assembly level. A passenger car and an SUV were used in the vehicle impact tests to investigate the differences in the impact response of the Flex-PLI due to the difference in car front shape. As shown in Figure 28, the vehicle tests were performed at 40 km/h, and the Flex-PLI was propelled into the laterally center part of the vehicle. In terms of instrumentation, three and four strain gauges were affixed to the bone core of the thigh and leg, respectively, as shown in Figure 29. The bending moment at each position on the thigh and leg (Thigh 1-3, Leg 1-4) was calculated from the strain measured. The moment calculation was based on the separate quasi-static mid-shaft 3-point bending test where the correlation factor between the strain of each strain gauge and the moment calculated from the reaction force from one support multiplied by the distance between the strain gauge and the support was determined. In addition, the knee joint of the Flex-PLI features potentiometers to measure the displacement of both ends of the ligament cable

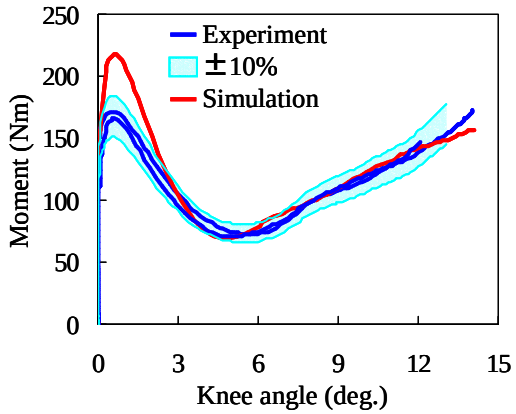

Figure 27. Comparison of moment-knee angle response of knee joint between experiment and simulation

relative to the tibial and femoral condyle. In order to compare the results of those measurements with the computer simulation results, Section Fore in PAM-CRASH^{TM} was set at each position of the strain gauges to provide bending moment at each cross-section. In the model, each set of the knee cable and knee springs was modeled as a single bar element and force-elongation property that corresponds to the stiffness of the combination of the two knee springs was applied to it, the displacement of the ends of the knee springs was automatically obtained by looking at the elongation of the bar element. Thus, the elongation of the bar element from the computer simulation was directly compared with the displacement of the ends of the knee spring in the experiment. Figure 30 compares the kinematics of the Flex-PLI between the computer simulation and experiment for both the passenger car and the SUV. As seen from the test results for the passenger car, the thigh and leg were significantly deformed around the knee joint, then the thigh leans onto the hood, and the leg is bounced off the bumper. The computer simulation model reproduces the same behavior as that obtained experimentally. In the case of the SUV, since the hood edge is high relative to that of the passenger car, the hood and the grille of the SUV can restrain the thigh. This results in smaller deflection of the thigh compared to that of a passenger car. However, the leg enters the space beneath the bumper, resulting in greater deflection in the lower end of the leg. The computer simulation model also shows deflection of the thigh and leg similar to that of the experimental results. It was therefore confirmed that the characteristic kinematics resulting from the difference in the front shape of the passenger car and SUV can be reproduced.

Figure 31 shows a comparison between the results of the experiment and computer simulation for the maximum values of the bending moment of the thigh and leg. While the simulation result for Thigh-1 in the case of the passenger car is higher than the test results, the simulation results for other parts are within ±10% of the test results, indicating good agreement. Because Thigh-1 is struck by the hood edge, deforms about the hood edge, and consequently generate bending moment, the hood edge of the vehicle model is most likely more rigid relative to that of an actual vehicle considering the fact that the FE model for the passenger car used in this study was for a slightly different model from the car used in the tests. Therefore, better agreement between the test results and computer simulation results for Thigh-1 should be able to be obtained by improving the model for the parts in the vicinity of the hood edge. However, since the objective of this study was to validate the Flex-PLI model, improved accuracy of the vehicle model was considered as an issue for future study. In the case of SUV, the trend of the simulation results for the bending moment of both the thigh and leg agreed with that of the test results, and the simulation results were within ±10% of the test results. This indicates good quantitative agreement between the test results and computer simulation results. Figure 32 shows a comparison of the maximum elongation of the bar element that represents the knee cable and knee springs (for the experiment, this is equivalent to the displacement of the ends of the knee springs) between the experiment and computer simulation. The simulation results for the elongation of the knee cables were within ±10% of the test results for both the passenger car and SUV, indicating good accuracy.

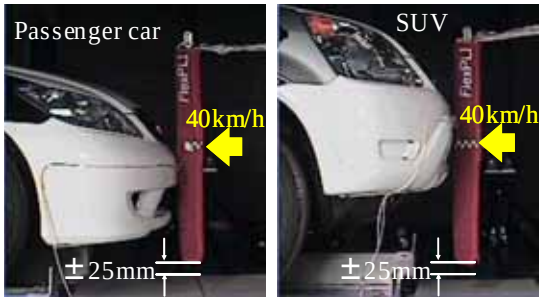

Figure 28. Vehicles impact test setup

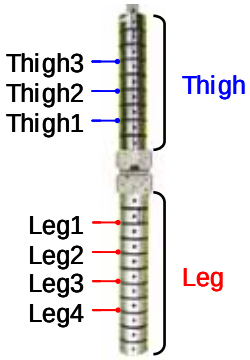

Figure 29. Strain gauges attachment position for thigh and leg

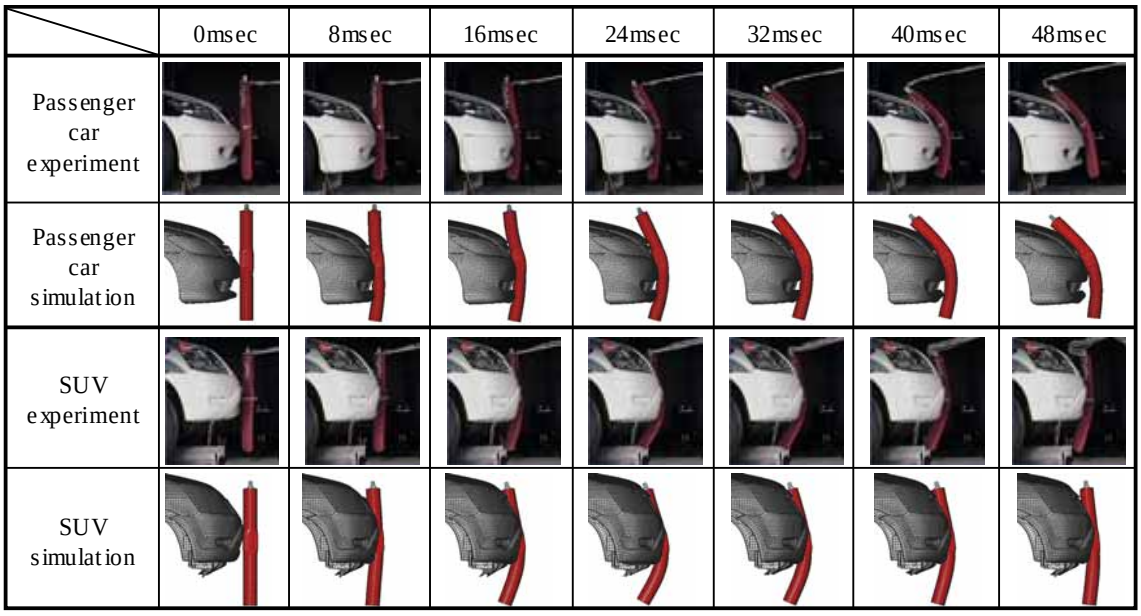

Figure 30. Comparison of the Flex-PLI motion between experiment and simulation for vehicle impact test

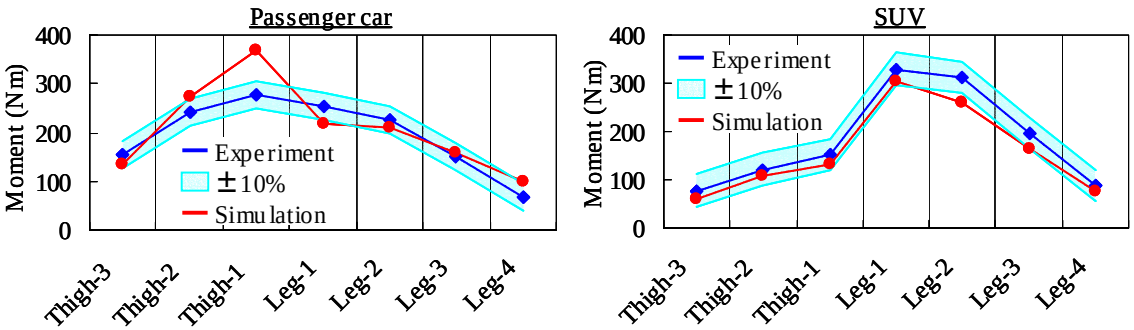

Figure 31. Comparison of peak bending moment for thigh and leg between experiment and simulation

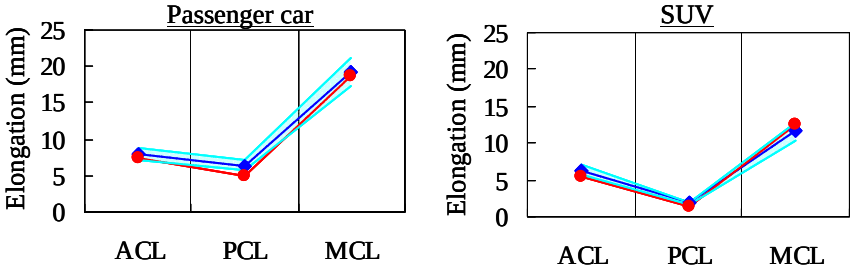

Figure 32. Comparison of knee spring expand between experiment and simulation

CONCLUSION

In order to reduce the CPU time for the bone core model in the bony structure of the thigh and leg, a model was made by calculating the areal moment of inertia from the cross-section of the bone core, and by replacing the cross section with more simple one yet conserving the areal moment of inertia. As a result, it was possible to reduce the CPU time without compromising the accuracy of the model. In addition, the force-deflection property obtained from the 3-point bending tests for the bone core were compared with the simulation results, and the comparison showed that there was good agreement between the results even with the simplified cross-section of the bone core.

Regarding the resin material characterization for each part, quasi-static and dynamic compression tests were carried out to determine the material property. Because the strain rate dependency of the material for each resin material was observed from these results, the strain rate dependency was incorporated in the material model. Consequently, the results of the quasi-static and dynamic compression tests agreed well with the simulation results, confirming that the force-deflection response of the resin material could be reproduced.

An FE model that accurately reproduced the geometry of the parts based on the Flex-PLI drawing was validated in 3-point lateral bending of the thigh and leg and 4-point lateral bending of the knee joint. It was found that the simulation results for both the thigh, leg and knee joint fell within ±10% of the test results. This indicates good accuracy of the model as well as validity of the modeling technique.

In the validation of the Flex-PLI assembly model, vehicle impact tests were performed. The kinematics obtained from the tests with the passenger car and the SUV, which have different front shape, was compared with that of the model. As a result, it was confirmed that the model reproduced the characteristic kinematics of the Flex-PLI due to the difference in the vehicle front shape. Also, the maximum bending moment of the thigh and leg as well as the maximum elongation of the knee cables were compared between the experiment and computer simulation. The results showed that there was quantitative agreement between the experiment and computer simulation. However, in the reproduction of the vehicle impact test, a highly accurate vehicle model is required. Thus, more accurate modeling for the parts in the front of the vehicle as well as improvement in the accuracy of the material model for those parts are issues for future study.

ACKNOWLEDGMENTS

The authors would like to express their sincere thanks to Mr. Atsuhiro Konosu of the Japan Automobile Research Institute, who developed the Flex-PLI, for his valuable guidance in assembling the Flex-PLI, and for his kind cooperation with the tests carried out during the development of the Flex-PLI model.l.

REFERENCES

[1] 1995. “International road traffic and accident database.”

[2] European enhanced vehicle-safety committee. 1998. “EEVC working group 17 report, Improved test methods to evaluate pedestrian protection afforded by passenger cars.”

[3] Matsui Y. and Sasaki A. etc. 1999. “Impact response and biofidelity of pedestrian legform impactor.” IRCOBI.

[4] Konosu A. and Ishikawa H. etc. 2001. “Reconsideration of injury criteria for pedestrian subsystem legform test － Problem of rigid legform impactor －” 17th ESV conference, Paper number 263.

[5] Takahashi Y. and Kikuchi Y. 2001. “Biofidelity of test devices and validity criteria for evaluating knee injures to pedestrians.” 17th ESV conference, Paper number 373.

[6] Konosu A. and Tanahashi M. 2003. “Development of a biofidelic flexible pedestrian legform impactor.” Stapp, Paper number 03S-09.

[7] Konosu A. and Tanahashi M. 2004. “Development of a biofidelic legform impactor – application in a car-pedestrian subsystem test.” SAE, Paper number 04B-22.

[8] Konosu A. and Tanahashi M. 2005. “Development of a biofodelic flexible pedestrian leg-form impactor (Flex-PLI 2004) and evaluation of its biofidelity at the component level and at the assembly level.” SAE, Paper number 05B-161.

[9] Japan automobile manufacturers association, inc. 2004. “Flex-PLI 2004 plan.”

[10] 2002. “Pam system international, PAM-CRASH™ PAM-SAFE™ version 2002 notes manual.”

[11] 2002. “Pam system international, PAM-CRASH™ PAM-SAFE™ version 2002 reference manual.”

[12] 2002. “Pam system international, PAM-GENERIS™ for PAM-CRASH™ & PAM-SAFE™ version 2001.1 reference manual.”